Handbook of Research on Advancements in Robotics and Mechatronics

Maki K. Habib
The American University in Cairo, Egypt

A volume in the Advances in Computational Intelligence and Robotics (ACIR) Book Series

ENGINEERING SCIENCE REFERENCE
An Imprint of IGI Global

Managing Director: Lindsay Johnston
Managing Editor: Austin DeMarco
Director of Intellectual Property & Contracts: Jan Travers
Acquisitions Editor: Kayla Wolfe
Production Editor: Christina Henning
Development Editor: Austin DeMarco
Typesetter: Amanda Smith
Cover Design: Jason Mull

Published in the United States of America by
Engineering Science Reference (an imprint of IGI Global)
701 E. Chocolate Avenue
Hershey PA, USA 17033
Tel: 717-533-8845
Fax: 717-533-8661
E-mail: cust@igi-global.com
Web site: http://www.igi-global.com

Library of Congress Cataloging-in-Publication Data

Handbook of research on advancements in robotics and mechatronics / Maki K. Habib, editor.
pages cm
Includes bibliographical references and index.
ISBN 978-1-4666-7387-8 (hardcover) -- ISBN 978-1-4666-7388-5 (ebook) -- ISBN 978-1-4666-7390-8 (print & perpetual access) 1. Robotics--Technological innovations. 2. Mechatronics--Technological innovations. I. Habib, Maki K., 1955- editor.
TJ211.H264 2015
629.8'92--dc23

2014039999

This book is published in the IGI Global book series Advances in Computational Intelligence and Robotics (ACIR) (ISSN: 2327-0411; eISSN: 2327-042X)

British Cataloguing in Publication Data
A Cataloguing in Publication record for this book is available from the British Library.

Chapter 16
Control of a Biomimetic Robot Hand Finger: Classical, Robust, and Intelligent Approaches

Yunus Ziya Arslan
Istanbul University, Turkey

Yener Taskin
Istanbul University, Turkey

Yuksel Hacioglu
Istanbul University, Turkey

Nurkan Yagiz
Istanbul University, Turkey

ABSTRACT

Due to the dexterous manipulation capability and low metabolic energy consumption property of the human hand, many robotic hands were designed and manufactured that are inspired from the human hand. One of the technical challenges in designing biomimetic robot hands is the control scheme. The control algorithm used in a robot hand is expected to ensure the tracking of reference trajectories of fingertips and joint angles with high accuracy, reliability, and smoothness. In this chapter, trajectory-tracking performances of different types of widely used control strategies (i.e. classical, robust, and intelligent controllers) are comparatively evaluated. To accomplish this evaluation, PID, sliding mode, and fuzzy logic controllers are implemented on a biomimetic robot hand finger model and simulation results are quantitatively analyzed. Pros and cons of the corresponding control algorithms are also discussed.

1. INTRODUCTION

Due to the high functional properties of biological systems, many scientists were inspired by the nature to find solutions to problems in medicine and engineering. There have been many important advancements in the biologically inspired technology that is especially developed in the area of robotics and mechatronics (Habib, 2007; Habib, 2011). Human inspired robotic technology has made a significant improvement over the past two decades (Schaal, 1999; Breazeal and Scassellati, 2002; Chen et al., 2011; Chen and Huang, 2012). Especially, there have been many promising advancements in the field

DOI: 10.4018/978-1-4666-7387-8.ch016

of bio-inspired robotics hands. For the state of the art and current trends in the development of dexterous robotic hands, refer to the review articles of Shimago (1996), Biagiotti et al. (2004) and Mattar (2013). One of the main challenges in executing manipulation task is how to control the robot hands such that they can produce motions with the same dexterity and intuition as human hands (Al-Gallaf et al., 1993). To handle the motion control problem of humanoid robotic hands, different types of control algorithms were introduced and implemented (Pons et al., 1999; Hacioglu et al., 2008; Arslan et al., 2009). In this study, to evaluate the trajectory tracking performances of widely used control methods, namely PID, sliding mode and fuzzy logic controllers were implemented on a biomimetic robot hand finger model and simulation results were comparatively discussed. Because of the similar biomechanical properties and kinematic structures of the hand fingers to each other's except thump, motion control of only one finger, i.e. index finger has been considered. Hence, in this study, analyzing the flexion motion of the human hand is reduced to examine the single finger motion.

Since it has relatively simple algorithm for application and provide successful performance, PID controller is probably the most widely used control approach in industrial applications (Ang et al., 2005; Åström and Hägglund, 2006; Åström and Murray, 2008). The PID controller algorithm involves three separate constant parameters: the proportional gain, the integral and derivative times. The weighted sum of three actions is used to adjust the control process. For specific control tasks, those parameters are tuned according to the requirements of the process (Kelly, 1995).

Due to its invariance properties, sliding mode control (SMC) is a widely used robust control method, especially in the field of robotics (Yagiz et al., 2007; Feng et al., 2002; Engeberg and Meek, 2013). It is a special class of variable structure control systems in which the control law is deliberately changed during the control process according to some predefined rules depending on the states of the system (Edwards and Spurgeon, 1998). The fundamental concept of the SMC is to drive the system states to the so-called sliding surface and then keep the system within a neighborhood of that surface (Utkin, 1977). During the sliding motion, the system is insensitive to parameter variations and external disturbances (Yagiz et al., 2010).

Fuzzy logic control (FLC) is a knowledge-based control method and it is based on the fuzzy set theory (Zadeh, 1965). Because it has applicability to systems with unknown mathematical model and it has a rule-based structure, this control approach has become widespread (Feng, 2006; Hacioglu et al., 2011). In this method, the experience-based knowledge can be expressed by fuzzy rules and they are used for the control signal calculations. Fuzzy logic has the advantage comparing with other machine learning systems such as neural networks that the solution of the control problem can be defined in such a way that human operator can understand; therefore operator's experience can be used in the design of the controller. Because of these attractive properties, fuzzy logic has been used in wide range of control applications (Taskin et al., 2007; Arslan et al., 2008; Yagiz and Hacioglu, 2009).

2. PHYSICAL MODEL OF THE BIOMIMETIC FINGER

The biomimetic hand finger, on which the controller methods were applied, was modeled as a kinematic chain of three cylindrical links that mimics the inertial properties of the proximal, middle and distal phalanges of the index finger (Figure 1). Spherical elements were added to the articulations of the model to represent the joint masses of the finger.

Figure 1. Physical model of the biomimetic robot hand finger

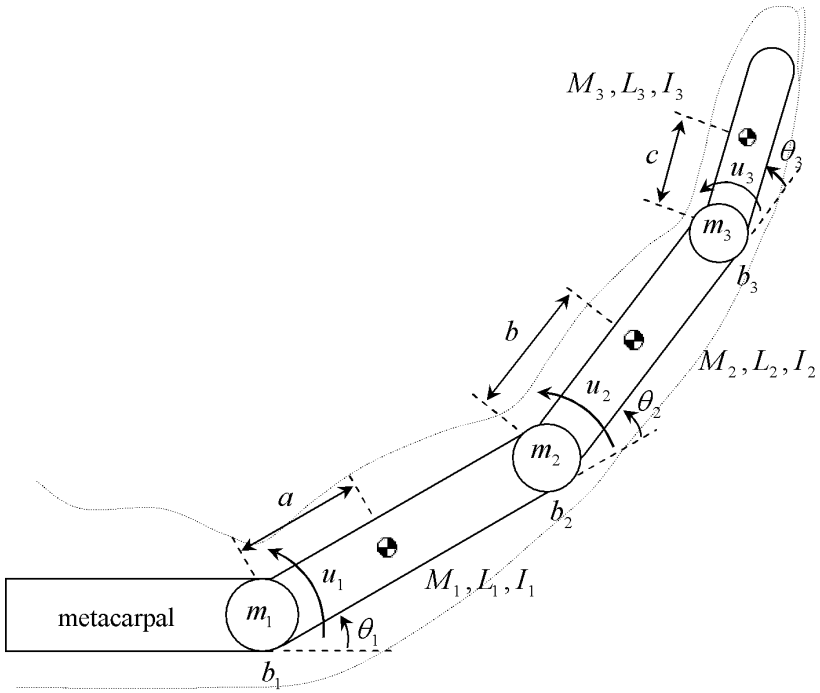

In the model, u_i stands for the control torque acting on the related joint, which is produced by the corresponding control algorithm and θ_i is the relative joint angle. The link lengths of model were extracted using camera images of a human hand index finger during its closing motion. In addition, the diameters of links and joints were determined according to an x-ray image of a real human hand. Mass of the links and joints were calculated by taking the bone density of 1.9 g/cm^3 into account (Weghe *et al.* 2004). Numerical values of the link mass (M_i), link length (L_i), mass moment of inertia of link (I_i), distances of the mass center of the first (a), second (b) and third link (c), masses of joints (m_i), and viscous friction at each revolute joint (b_i) were given in Appendix A (*i=1,2,3*).

Equations of motion of the finger model were obtained by using Lagrange approach and given in vector-matrix form as below.

$$\left[M(\theta)\right]\ddot{\theta} + \boldsymbol{C}(\theta,\dot{\theta}) + \boldsymbol{G}(\theta) = \boldsymbol{u} - \boldsymbol{F} \tag{1}$$

where $\left[M(\theta)\right]$ is $n \times n$ mass matrix of the finger, $\boldsymbol{C}(\theta,\dot{\theta})$ is $n \times 1$ vector and includes the coriolis and centrifugal terms, $\boldsymbol{G}(\theta)$ is $n \times 1$ vector of the gravity terms, $\boldsymbol{u}$ is $n \times 1$ generalized torque vector and $\boldsymbol{F}$ is $n \times 1$ disturbance torque vector. To test the robust characteristic of the designed controllers, a resistive torque was applied to the proximal interphalangeal joint (joint 2) as an unexpected joint friction fault (Figure 2.a). Additionally, it was considered that the fingertip touched a soft object towards end of the motion, which did not prevent the completion of the flexion movement (Figure 2.b). Explicit form of Equation (1) was given in Appendix B.

Figure 2. a) Resistive torque applied to joint 2; b) disturbance torques applied to the joints

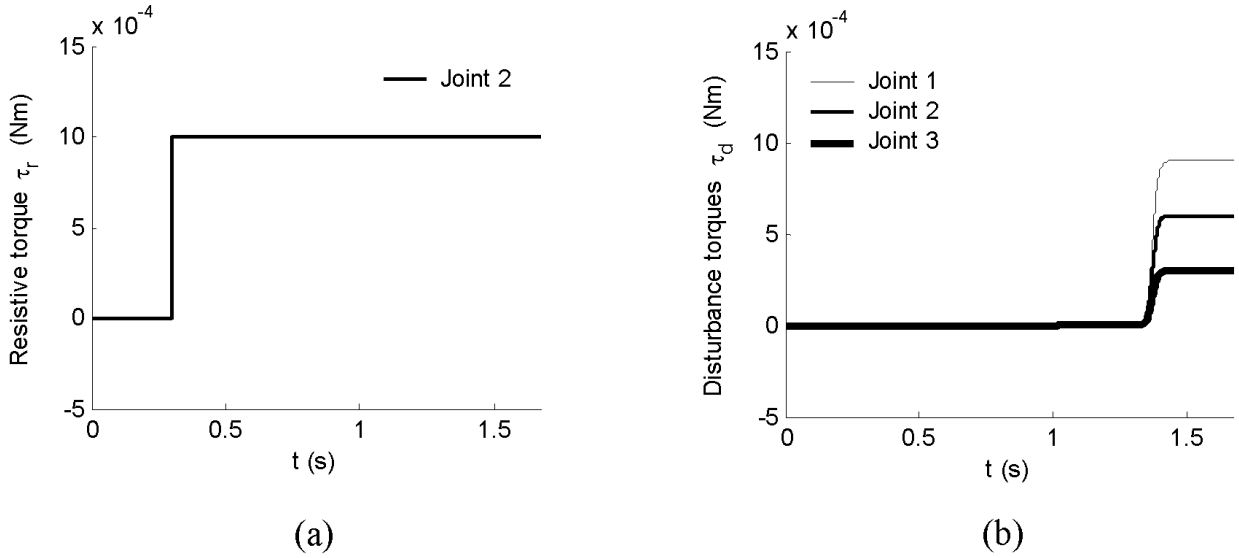

Figure 3. Video images of finger flexion movement used for extracting the finger trajectory

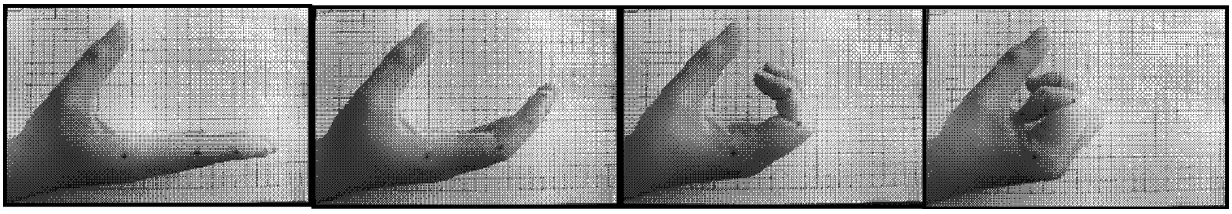

3. TRAJECTORY PLANNING

The biomimetic finger model was aimed to simulate the natural flexion movement of the human finger. To do so, trajectory of the finger model was planned using video images which were recorded during flexion movement of index finger (Figure 3). The recorded video was split into frames with 0.08 second time intervals. Then, these frames were exported into a computer aided design program. Joint angles were manually digitized according to the points which were marked on the center of joints.

In order to have continuous and smooth joint angles as reference, sixth order polynomials were fitted to the joint angle data. By using the angles as input for the forward kinematics, the motion of the end of the distal link, that is, the trajectory of the finger model was obtained. The obtained polynomials were used as reference for the controllers through the numerical analysis of the finger model. The obtained reference joint angles and trajectory of the fingertip is given in Figure 4.

Figure 4. References for joint angles of (a) joint 1, (b) joint 2, and (c) joint 3; (d) trajectory of the finger tip for closing motion

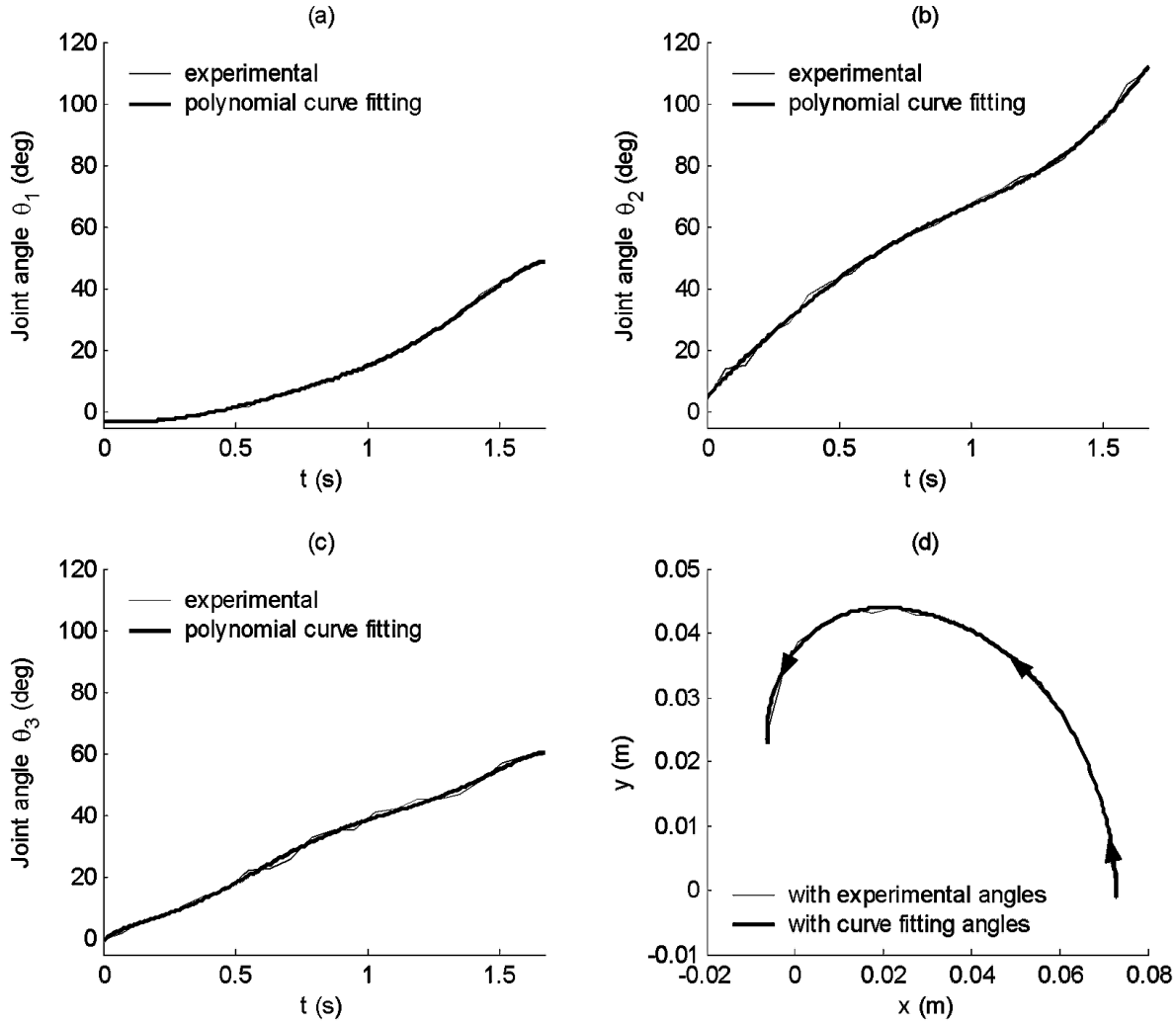

4. CONTROL APPLICATIONS

Classical Control Application: PID

What is meant by classical control application is the use of the proportional-integral-derivative (PID) controller in feedback control issue of a robotic hand finger. PID controller is also known as three term control algorithm and used very widely in process control industry. Even if three term controller was first introduced in 1936 by the Taylor Instrument Company, Nicolas Minorsky had analyzed the properties of the three term controller in 1922 (Bennett, 1984). In 1942, Ziegler and Nichols published a

paper (Ziegler and Nichols, 1942) where they described two methods for tuning the parameters of P, PI and PID controllers. These two methods are known as the Ziegler-Nichols' closed loop method, and the Ziegler-Nichols' open loop method. Based on a survey of over eleven thousand controllers (Åström and Murray, 2008), more than 90% of the control and automation applications are done by PID controllers since it is effective and easy to implement. The main factor for the choice of controller is that it has a simpler structure and gives satisfactory results by setting a small number of parameters which can be explained physically.

PID controller structure includes the effects of present, past and future errors as inputs and the control signal as the output of the controller that can be seen in Equation (2) and in Figure (5). K_P, T_I and T_D are positive PID parameters, which denote proportional gain, integral time and derivative time respectively.

$$u(t) = K_P \left(e(t) + \frac{1}{T_I} \int e(\tau) d\tau + T_D \frac{de(t)}{dt} \right) \tag{2}$$

In the control law, the term that includes the proportional gain K_P depends on the present error. The sum of past errors is obtained by the term including integral gain K_P / T_I, and the term with derivative gain $K_P T_D$ gives an estimation of future errors. Therefore, the control signal is composed of the sum of these three actions. Proportional gain is applied to the error between reference and measured or calculated state output. Integral and derivative gains are also applied to the integral and derivative of error between reference and state output respectively. While larger values of proportional gain give faster response, instability and oscillations can occur for very large values of proportional gain. Additionally, proportional gain cannot be adequate to remove steady state error by itself. However integral gain can eliminate the steady state error and also larger values of integral gain remove steady state error rapidly. On the other hand derivative gain has the ability to decrease overshoot, but gives slower transient response for larger values. It should be noted that the differentiation of the error may cause instability due to signal noise amplification.

In order to tune the PID controller, the trial and error method, which is also known as manual tuning, was preferred. The tuning was begun with the proportional term till a sufficient response is get from the closed loop system. Then, integral term was increased to remove steady state error. Finally, derivative term was tuned to reach reference quickly by decreasing the settling time.

Figure 5. PID controller structure

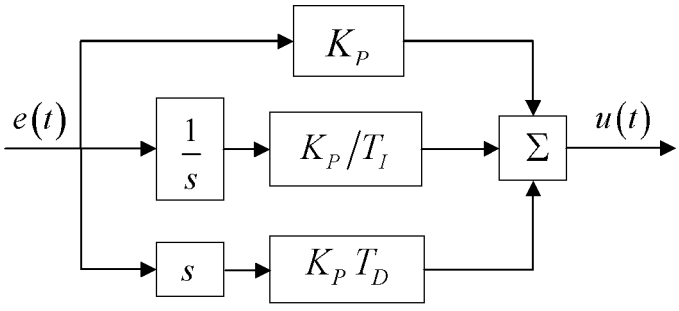

For the implementation of the proposed PID control, heuristics-based tuning was followed for each local PID controller independently. Although there has been a long standing belief that PID control is inadequate to cope with highly nonlinear systems (Cervantes and Ramirez, 2001), Rigatos and Siano (2011) proposed a robust power system stabilizer using Kharitonov's extremal gain margin theory. Similarly, a class of stabilizing decentralized PID controllers was determined for an n-link robot manipulator using Kharitonov's theorem and boundary stability condition by Leena and Ray (2012). Cervantes and Ramirez (2001) also showed semiglobal stability with arbitrary small output tracking error of robot manipulators under classical PID control.

It is worth noting that all the states were assumed to be measured and available for feedback during the PID control design. In fact, this will be also the case for the SMC and FLC designs. On the other hand, although it is not in the scope of this study, it is possible to implement the control schemes with observers for minimum number of sensor measurements and estimation of velocities and forces (Rigatos, 2012; Rigatos, 2014).

Robust Control Application: Sliding Mode Control (SMC)

As a variable structure system, in sliding mode controlled systems, control action is intentionally changed depending on the states of the system according to certain predefined rules (Edwards and Spurgeon, 1998). By doing so, the system is driven towards a sliding surface and constrained to stay over that surface. Then system states converge to zero by sliding on that surface. In fact, there are mainly two stages during the design of this controller. First, sliding surface is defined in the state space, and second, the control law is derived that will construct and maintain such a sliding motion. Since the control law is based on the Lyapunov's direct method, stability of the system is guaranteed.

The equation of motion of the finger model can be arranged in the state space form as

$$\dot{\boldsymbol{x}} = \boldsymbol{f}\left(x\right) + \left[B\right]\boldsymbol{u} \tag{3}$$

Here $\boldsymbol{x} = [x_1, ..., x_n, x_{n+1}, ..., x_{2n}]^T$. The second half of the states are the time derivatives of the first half and $2n$ is the number of the states, $\boldsymbol{f}(x)$ is $2n \times 1$ vector that includes the non-linear part of the equations without control inputs, $\boldsymbol{u}$ is $n \times 1$ control torque input vector, $[B]$ is $2n \times n$ control input matrix. The sliding surface is defined as,

$$\boldsymbol{\sigma} = \left[G\right]\boldsymbol{e} \tag{4}$$

Here $\boldsymbol{e} = \boldsymbol{x}_{\mathrm{r}} - \boldsymbol{x}$ is the difference between the reference value and system response, namely the tracking error, and $\left[G\right]$ includes the sliding surface slopes. Then:

$$\sigma_{\mathrm{i}} = \alpha_i \, e_{\mathrm{i}} + \dot{e}_{\mathrm{i}} \tag{5}$$

α_i represents the negative value of the each related sliding surface slope. For stability, following Lyapunov function candidate, which is proposed for a non-chattering action, has to be positive definite and its derivative has to be negative semi-definite.

$$\boldsymbol{V} = \frac{\boldsymbol{\sigma}^{\boldsymbol{T}}\boldsymbol{\sigma}}{2} > 0 \tag{6}$$

$$\frac{d\boldsymbol{V}}{dt} = \frac{\dot{\boldsymbol{\sigma}}^{\boldsymbol{T}}\boldsymbol{\sigma}}{2} + \frac{\boldsymbol{\sigma}^{\boldsymbol{T}}\dot{\boldsymbol{\sigma}}}{2} \leq 0 \tag{7}$$

If the limit condition is applied to Equation (7), the sliding mode condition is obtained as

$$\frac{d\boldsymbol{\sigma}}{dt} = \frac{d\boldsymbol{\Phi}(t)}{dt} - [G]\frac{d\boldsymbol{x}}{dt} = 0 \tag{8}$$

where

$$\boldsymbol{\Phi}\left(t\right) = \left[G\right]\boldsymbol{x}_r \tag{9}$$

From Equations (3) and (8)

$$\frac{d\boldsymbol{\Phi}(t)}{dt} - [G]\left(\boldsymbol{f}\left(x\right) + \left[B\right]\boldsymbol{u}_{eq}\right) = 0 \tag{10}$$

where $\boldsymbol{u}_{eq}$ is the equivalent control torque input vector for the limit condition. Finally, the equivalent control torque input is obtained as

$$\boldsymbol{u}_{eq} = \left[GB\right]^{-1}\left(\frac{d\boldsymbol{\Phi}\left(t\right)}{dt} - \left[G\right]\boldsymbol{f}\left(x\right)\right) \tag{11}$$

Since equivalent control is valid only on the sliding surface, an additional term should be defined to drive the system to the surface. For this purpose derivative of the Lyapunov function is selected as follows.

$$\dot{\boldsymbol{V}} = -\boldsymbol{\sigma}^{\mathrm{T}}\left[\Gamma\right]\boldsymbol{\sigma} < 0 \tag{12}$$

By equating the Equations (7) and (12)

$$\boldsymbol{\sigma}^{\mathrm{T}}\dot{\boldsymbol{\sigma}} = -\boldsymbol{\sigma}^{\mathrm{T}}\left[\Gamma\right]\boldsymbol{\sigma} \tag{13}$$

$$\frac{d\boldsymbol{\sigma}}{dt} + \left[\Gamma\right]\boldsymbol{\sigma} = 0 \tag{14}$$

by using the $\dot{\mathbf{x}}$ from Equation (3) and taking the derivative of Equation (4)

$$\frac{d\boldsymbol{\Phi}(t)}{dt} - [G]\left(\boldsymbol{f}\left(x\right) + \left[B\right]\boldsymbol{u}\right) + \left[\Gamma\right]\boldsymbol{\sigma} = 0 \tag{15}$$

by using the control law for equivalent control in Equation (11) the total control input is found to be

$$\boldsymbol{u} = \boldsymbol{u}_{eq} + \left[GB\right]^{-1}\left[\Gamma\right]\boldsymbol{\sigma} \tag{16}$$

With the designed control law (16), the derivative of the positive definite Lyapunov function (6) with respect to time along the system trajectories (3) is negative definite as selected in Equation (12). Therefore, the system is asymptotically stable and sliding variable is regulated to zero, that is, $\boldsymbol{\sigma} \to 0$ as $t \to \infty$. Then, positive definite values of α_i provide stable sliding motion on the sliding surface, and tracking error variable is also regulated to zero, that is, $\boldsymbol{e} \to 0$ as $t \to \infty$.

$\left[GB\right]^{-1}$ is always invertible and equals to mass matrix for mechanical systems. The control gain matrix $\left[\Gamma\right]$ is a positive definite matrix and its entries are decided by trial at the design stage. However, if the knowledge concerning on $\boldsymbol{f}\left(x\right)$ and $\left[B\right]$ is poor, then calculated equivalent control inputs will be different from the needed equivalent control inputs. Therefore, in this study, it was assumed that the equivalent control is the average of the total control. For estimation of the equivalent control, an averaging filter, here a low pass filter with time constant τ, was designed as follows.

$$\hat{\boldsymbol{u}}_{eq} = \frac{1}{\tau s + 1}\boldsymbol{u} \tag{17}$$

As a result the non-chattering control torque input can be given as

$$\boldsymbol{u} = \hat{\boldsymbol{u}}_{eq} + \left[GB\right]^{-1}\left[\Gamma\right]\boldsymbol{\sigma} \tag{18}$$

The main idea in using a low-pass filter is that the low frequencies determine the characteristics of the signal and high frequencies come from the unmodeled dynamics. The time constant of the low-pass filter should be sufficiently small to preserve the slow component undistorted and it should be large enough to eliminate the high-frequency component. Then, the output of the low-pass filter tends to the equivalent control (Utkin et al., 1999). Thus, stability of the system is preserved.

Intelligent Control Application: Fuzzy Logic Control (FLC)

In FLC, linguistic expressions are used for the controller design to generate a knowledge-based control method which consists of the intuition of human operators or experts. These heuristic decision rules are generally in the following form for a system with two inputs and single output:

If (x is X) and (y is Y) Then (u is U) (19)

The fuzzification, inference and defuzzification are the main steps in FLC applications. In the first step, membership functions and their ranges are established for the variables used in the control design. In the second step, the controller output is set according to predefined rules which are based on the knowledge about system characteristics coming from human operators or experts. In the last step, the output values could not be used directly, thus a suitable defuzzification method is chosen to convert the output to a crisp value. There are different defuzzification methods available in the literature such as, maximum membership principle, weighted average method, centroid method; while the last one is often preferred by the researchers (Arslan et al., 2008) and it was used in this study.

In order to control the movement of the robotic hand finger, a PD type fuzzy logic controller was used in the study. Structure of the controller is shown in Figure 6. In the control structure, error e_N and its derivative $\dot{e}_N$ were used as inputs. The output of the PD-type fuzzy controller was the control signal u_N.

The fuzzification of the input and output variables was done by Gaussian membership functions. Membership functions for the error e_N and its derivative $\dot{e}_N$ are shown in Figure 7a and membership functions for the output u_N are shown in Figure 7b. In the membership functions, *NB*, *NM*, *NS*, *Z*, *PS*, *PM* and *PB* denote negative big, negative medium, negative small, zero, positive small, positive medium and positive big, respectively. All the membership functions were defined on the [-1,1] closed interval. SF_e and SF_{de} are the input scaling factors. SF_u is the output scaling factor of the PD-type fuzzy logic controller. All these scaling factors were used in order to map the related crisp values to their fuzzy universe of discourse. In order to obtain a good tracking performance of the controller, trial and error based heuristic tuning was carried out to determine the scaling factors of the controller. Relations between the input and output variables for the PD type controller were given below. The subscript *N* denotes the normalized variable in the equations.

Figure 6. General structure of the controller

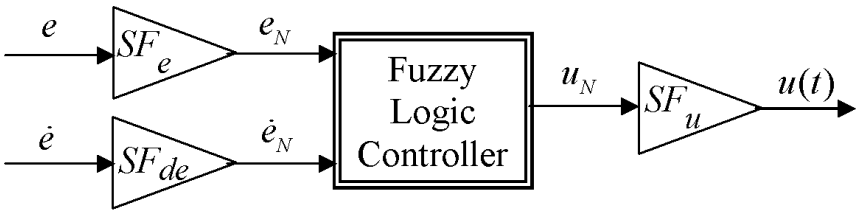

$$e_N = SF_e\, e \tag{20}$$

$$\dot{e}_N = SF_{de}\, \dot{e} \tag{21}$$

$$u(t) = SF_u\, u_N \tag{22}$$

The output u_N was calculated by the rule table shown in Table 1 for the PD-type fuzzy logic controller.

Figure 7. Membership functions for a) input variables b) output variable

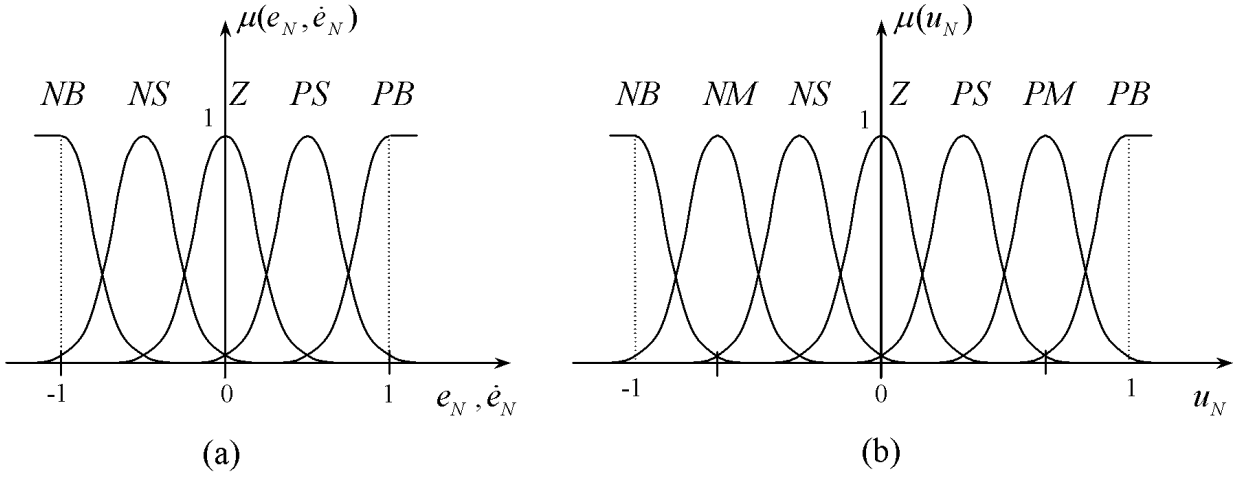

Table 1. Rule table for u_N

e_N \ $\dot{e}_N$	**NB**	**NS**	**Z**	**PS**	**PB**
NB	*NB*	*NB*	*NM*	*NS*	*Z*
NS	*NB*	*NM*	*NS*	*Z*	*PS*
Z	*NM*	*NS*	*Z*	*PS*	*PM*
PS	*NS*	*Z*	*PS*	*PM*	*PB*
PB	*Z*	*PS*	*PM*	*PB*	*PB*

The construction of rule base was done by the following approach:

Suppose that the system output is far from the desired output, i.e. e_N is *PB* and $\dot{e}_N$ is *Z* (Figure 8, case 1) then u_N is selected to be *PM* in order to decrease the error value and bring the system state to the desired value rapidly. In case 2, the e_N is *Z*, but it tends to increase due to the nonzero $\dot{e}_N$ thus, u_N should not be zero and it is selected to be *NM*. In case 3, both e_N and $\dot{e}_N$ are *Z*, which is the desired case and the system does not need any control input therefore, u_N is selected to be *Z*. The rules are in the following form for the PD-type fuzzy logic controller:

If e_N(*is PB*)	*and If* $\dot{e}_N$(*is Z*)	*Then* (u_N *is PM*)	*Case* 1	(23)
If e_N(*is Z*)	*and If* $\dot{e}_N$(*is NB*)	*Then* (u_N *is NM*)	*Case* 2	(24)
If e_N(*is Z*)	*and If* $\dot{e}_N$(*is Z*)	*Then* (u_N *is Z*)	*Case* 3	(25)

It is well known that conventional FLCs operate like SMCs with a boundary layer. It is considered that there is a sliding line along the diagonal of the fuzzy rule base and the control signal has opposite signs at the two sides. Thus, evidence about the stability of the closed-loop control system can be obtained by the analogy between conventional FLC and SMC (Palm, 1992). Design parameters of all three controllers were given in Appendix C.

5. NUMERICAL RESULTS AND DISCUSSION

The numerical results of biomimetic robot hand finger model with the designed PID, sliding mode and fuzzy logic controllers were presented in this section.

The error between the reference and simulated joint angles were calculated and given in Figure 9a for the PID controlled case. The time history of control torques was also given in Figure 9b. According to the results, maximum peak error, along with the maximum control torques, was observed in joint 1. Abrupt changes in tracking error and control torque were observed especially for the second joint of the finger model that is due to the resistive torque applied after 0.3 s of the motion. Similarly, sudden changes in tracking errors and control torques were observed towards the end of the motion that are due to the disturbance torques applied to the each finger joints.

Figure 8. Graphical representations for the sample rules

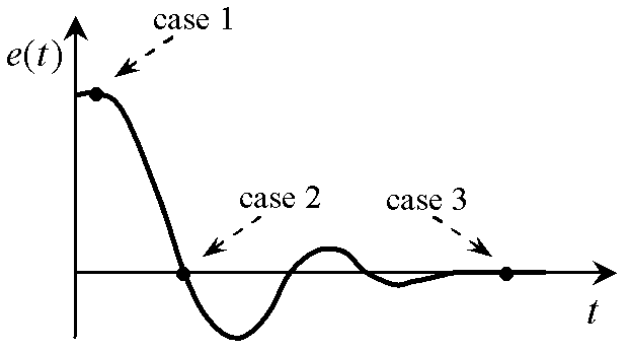

Figure 9. Time responses for PID controlled case: (a) tracking errors, (b) control torques

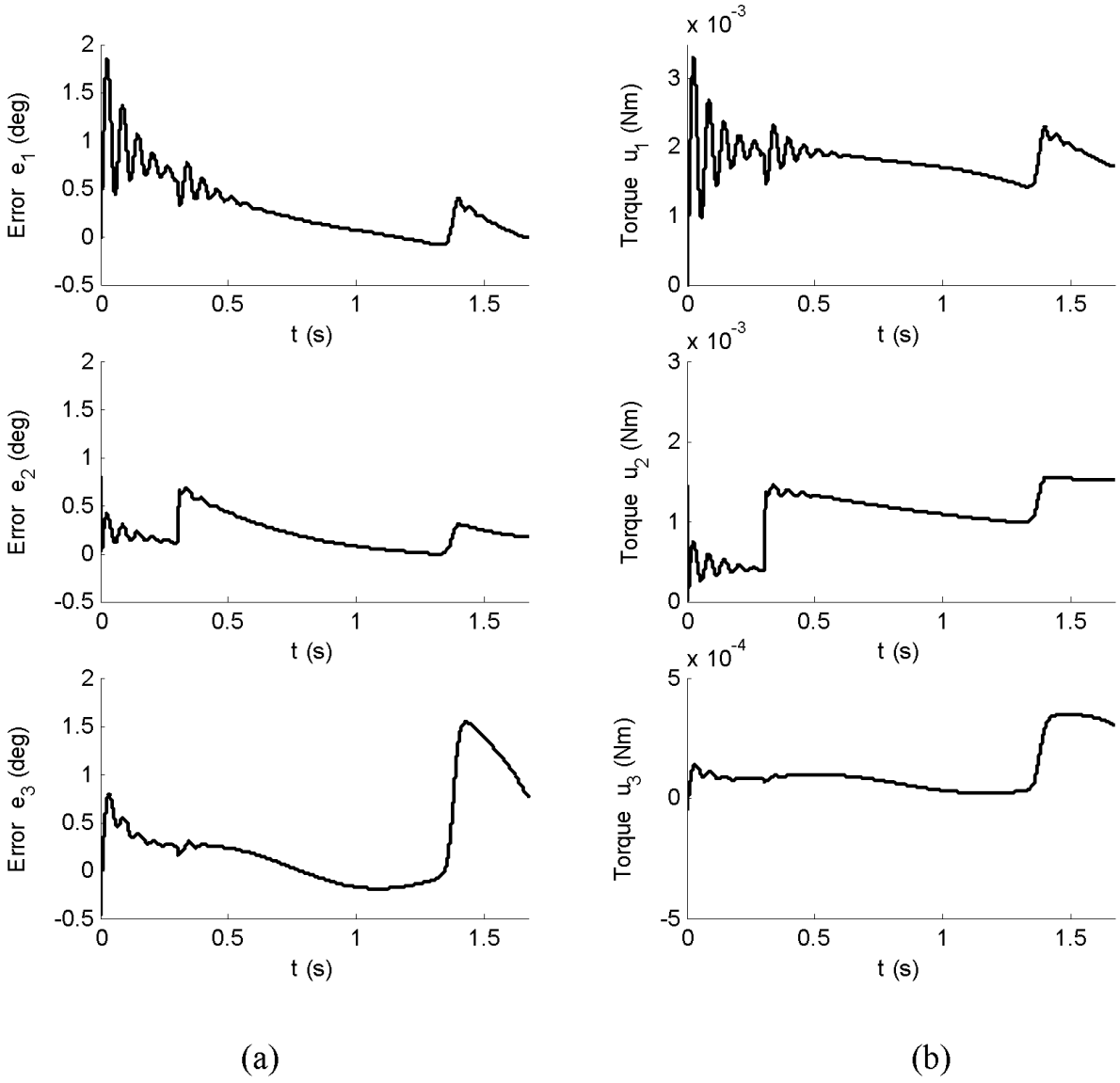

In Figure 10, the time histories of tracking errors and control torques for the sliding mode controlled case were presented. According to the results, maximum control torque was observed in joint 1 as it was for the PID case. Sudden changes in tracking errors and control torques were also observed for all joints of the finger model due to the applied disturbance torques and resistive torques. Also it was seen that the sliding mode controller recovered fast after application of the disturbances.

The tracking errors were given in Figure 11a for the fuzzy logic controlled case, and time history of control torques was also given in Figure 11b. According to the results, maximum control torque was observed in joint 1 as it was for the PID and sliding model controlled cases. Abrupt changes in tracking errors and control torques were also observed for all joints of the finger model due to the applied disturbance torques and resistive torque. It was seen that the FLC recovered fast after application of the disturbances.

Figure 10. Time responses for siding mode controlled case: (a) tracking errors. (b) control torques

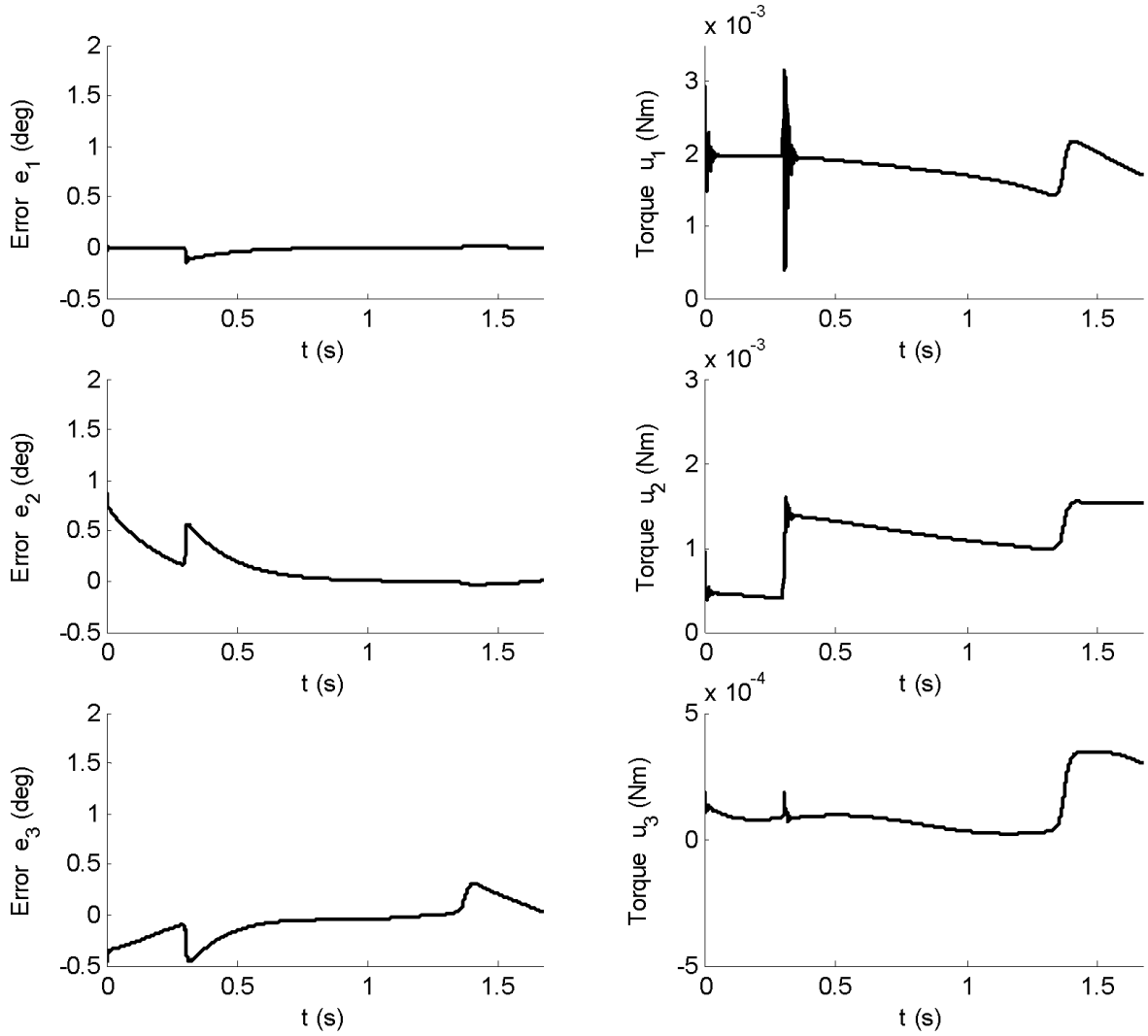

In order to quantitatively compare the trajectory tracking performances of the designed controllers, the Integral of Absolute Error (IAE) performance index was also calculated for related joint tracking errors and control torques, and tabulated in Table 2 and Table 3, respectively. The IAE (e_i) represents the tracking performance for the related link and IAE (u_i) denotes the control effort used for the actuation of the related link. It is observed that the IAE (e_i) takes minimum values for the two of the three joints with the sliding mode controller when compared with the PID and fuzzy logic controlled cases. On the other hand the IAE (u_i) values for all the joints are almost the same for all the controllers designed. Therefore it is deduced that sliding mode controlled case provide better performance than the PID and fuzzy controllers.

Figure 11. Time responses for fuzzy logic controlled case: (a) tracking errors, (b) control torques

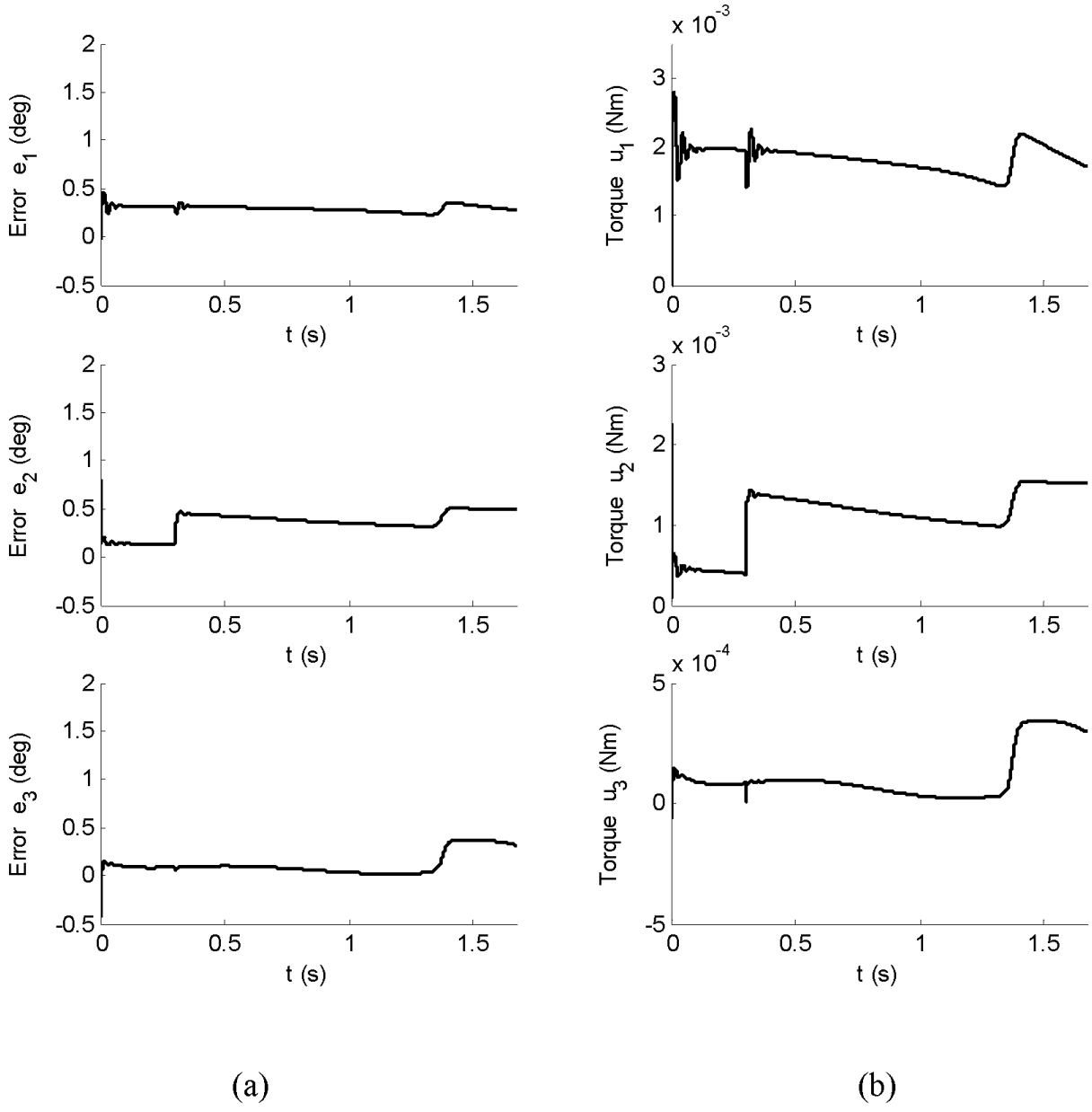

Table 2. IAE values for tracking errors

	IAE (e_1) (x10^{-3})	**IAE (e_2) (x10^{-3})**	**IAE (e_3) (x10^{-3})**
PID	9,1	6,2	11,3
Fuzzy	8,6	10,4	3,5
SMC	0,4	4	3,9

Table 3. IAE values for control torques

	IAE (u_1) (x10^{-3})	**IAE (u_2) (x10^{-3})**	**IAE (u_3) (x10^{-3})**
PID	2,791	1.658	0,1
Fuzzy	2,797	1,661	0,1
SMC	2,791	1,657	0,1

Figure 12. Comparison of the tracking errors under disturbance effects

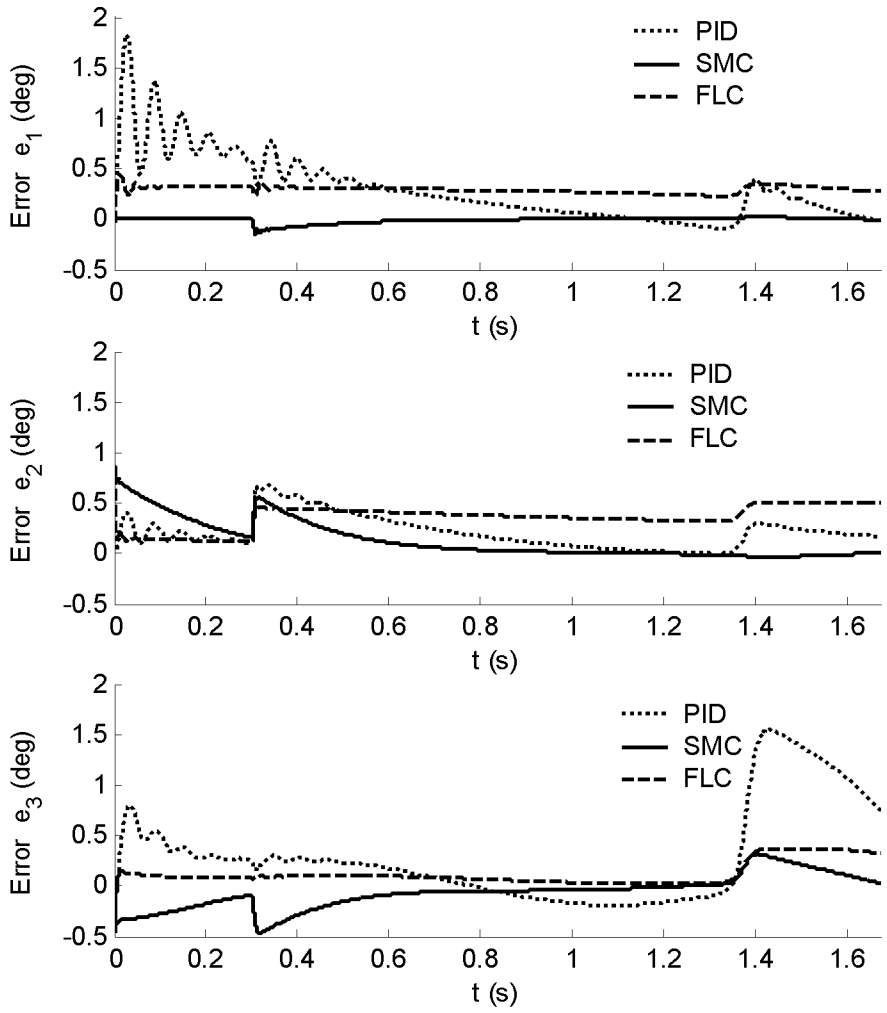

In order to compare the performances of the presented controllers in terms of stability and disturbance compensation, tracking errors were depicted together in Figure 12. According to the results, it is seen that all the controllers operate stable in the sense of Lyapunov, that is, all the tracking errors are bounded in the presence of disturbances. If the performances of the controllers in coping with the disturbances are investigated, it is observed that the SMC outperformed the PID and FLC, since the variation of the tracking errors obtained from SMC are less and tend to zero faster than those of PID and FLC.

6. CONCLUSION

To enable the robotic hands to achieve similar motion capabilities as human hand, various types of controllers have been employed. This chapter presents a comparative evaluation of widely used control strategies in robot hands. By taking both the trajectory tracking and joint torque production performances into account, it can be concluded that sliding mode controller outperformed PID and fuzzy logic controllers. However, numerical results were obtained from simulation applications and therefore, we should make this comment with caution, unless the corresponding controllers are applied to the real systems and the experimental results are analyzed.

REFERENCES

Al-Gallaf, E., Allen, A., & Warwick, K. (1993). A survey of multi-fingered robot hands: Issues and grasping achievements. *Mechatronics*, *3*(4), 465–491. doi:10.1016/0957-4158(93)90018-W

Ang, K. H., Chong, G., & Li, Y. (2005). PID control system analysis, design, and technology. *IEEE Transactions on Control Systems Technology*, *13*(4), 559–576. doi:10.1109/TCST.2005.847331

Arslan, Y. Z., Hacioglu, Y., & Yagiz, N. (2009). Fuzzy sliding mode control of a humanoid robot hand finger. *Expert Systems: International Journal of Knowledge Engineering and Neural Networks*, *26*(3), 291–303. doi:10.1111/j.1468-0394.2009.00488.x

Arslan, Y. Z., Yagiz, N., & Hacioglu, Y. (2008). Prosthetic hand finger control using fuzzy sliding modes. *Journal of Intelligent & Robotic Systems*, *52*(1), 121–138. doi:10.1007/s10846-008-9207-8

Åström, K. J., & Hägglund, T. (2006). Advanced PID control. ISA - The Instrumentation, Systems, and Automation Society.

Åström, K. J., & Murray, R. M. (2008). *Feedback systems: An introduction for scientists and engineers*. Princeton, NJ: Princeton University Press.

Bennett, S. (1984). Nicholas Minorsky and the automatic steering of ships. *IEEE Control Systems Magazine*, *4*(4), 10–15. doi:10.1109/MCS.1984.1104827

Biagiotti, L., Lotti, F., Melchiorri, C., & Vassura, G. (2004). *How far is the human hand? A review on anthropomorphic robotic end-effectors*. University of Bologna.

Breazeal, C., & Scassellati, B. (2002). Robots that imitate humans. *Trends in Cognitive Sciences*, *6*(11), 481–487. doi:10.1016/S1364-6613(02)02016-8 PMID:12457900

Cervantes, I., & Ramirez, J. A. (2001). On the PID tracking control of robot manipulators. *Systems & Control Letters*, *42*(1), 37–46. doi:10.1016/S0167-6911(00)00077-3

Chen, C. Y., & Huang, P. H. (2012). Review of an autonomous humanoid robot and its mechanical control. *Journal of Vibration and Control*, *18*(7), 973–982. doi:10.1177/1077546310395974

Chen, C. Y., Huang, P. H., & Chou, W. C. (2011). A critical review and improvement method on biped robot. *International Journal of Innovative Computing, Information, & Control*, *7*, 5245–5254.

Edwards, C., & Spurgeon, S. (1998). *Sliding mode control: Theory and applications*. London, UK: Taylor&Francis.

Engeberg, E. D., & Meek, S. G. (2013). Adaptive sliding mode control for prosthetic hands to simultaneously prevent slip and minimize deformation of grasped objects. *IEEE/ASME Transactions on Mechatronics*, *18*(1), 376–385. doi:10.1109/TMECH.2011.2179061

Feng, G. (2006). A survey on analysis and design of model-based fuzzy control systems. *IEEE Transactions on Fuzzy Systems*, *14*(5), 676–697. doi:10.1109/TFUZZ.2006.883415

Feng, Y., Yu, X., & Man, Z. (2002). Non-singular terminal sliding mode control of rigid manipulators. *Automatica*, *38*(12), 2159–2167. doi:10.1016/S0005-1098(02)00147-4

Habib, M. K. (2007). Mechatronics: A unifying interdisciplinary and intelligent engineering paradigm. *IEEE Industrial Electronics Magazine*, *1*(2), 12–24. doi:10.1109/MIE.2007.901480

Habib, M. K. (2011). Biomimetics: Innovation and robotics. *International Journal of Mechatronics and Manufacturing Systems*, *2*(2), 113–134. doi:10.1504/IJMMS.2011.039263

Hacioglu, Y., Arslan, Y. Z., & Yagiz, N. (2008). PI+PD type fuzzy logic controlled dual-arm robot in load transfer. *Strojniski Vestnik - Journal of Mechanical Engineering, 54*(5), 347-355.

Hacioglu, Y., Arslan, Y. Z., & Yagiz, N. (2011). MIMO fuzzy sliding mode controlled dual arm robot in load transportation. *Journal of the Franklin Institute*, *348*(8), 1886–1902. doi:10.1016/j.jfranklin.2011.05.009

Kelly, R. (1995). A tuning procedure for stable PID control of robot manipulators. *Robotica*, *13*(02), 141–148. doi:10.1017/S0263574700017641

Leena, G., & Ray, G. (2012). A set of decentralized PID controllers for an n-link robot manipulator. *Sadhana*, *37*(3), 405–423. doi:10.1007/s12046-012-0082-4

Mattar, E. (2013). A survey of bio-inspired robotics hands implementation: New directions in dexterous manipulation. *Robotics and Autonomous Systems*, *61*(5), 517–544. doi:10.1016/j.robot.2012.12.005

Palm, R. (1992). Sliding mode fuzzy control. In *Proceedings of the IEEE International Conference on Fuzzy Systems*. IEEE. doi:10.1109/FUZZY.1992.258681

Pons, J. L., Ceres, R., & Pfeiffer, F. (1999). Multifingered dextrous robotics hand design and control: A review. *Robotica*, *17*(6), 661–674. doi:10.1017/S0263574799001836

Rigatos, G. (2012). A robust nonlinear control approach for flexible-link robots using Kalman Filtering. *Journal of Cybernetics and Physics*, *1*(2), 134–143.

Rigatos, G. (2014). A differential flatness theory approach to observer-based adaptive fuzzy control of MIMO nonlinear dynamical systems. *Nonlinear Dynamics*, *76*(2), 1335–1354. doi:10.1007/s11071-013-1213-0

Rigatos, G., & Siano, P. (2011). Design of robust electric power system stabilizers using Kharitonov's theorem. *Mathematics and Computers in Simulation*, *82*(1), 181–191. doi:10.1016/j.matcom.2010.07.008

Schaal, S. (1999). Is imitation learning the route to humanoid robots? *Trends in Cognitive Sciences*, *3*(6), 233–242. doi:10.1016/S1364-6613(99)01327-3 PMID:10354577

Shimoga, K. B. (1996). Robot grasp synthesis algorithms: A Survey. *The International Journal of Robotics Research*, *15*(3), 230–266. doi:10.1177/027836499601500302

Taskin, Y., Hacioglu, Y., & Yagiz, N. (2007). The use of fuzzy-logic control to improve the ride comfort of vehicles. *Strojniski Vestnik-Journal of Mechanical Engineering*, *53*(4), 233–240.

Utkin, V., Guldner, J., & Shi, J. (1999). *Sliding mode control in electromechanical systems*. Taylor & Francis.

Utkin, V. I. (1977). Variable structure systems with sliding modes. *IEEE Transactions on Automatic Control*, *22*(2), 212–222. doi:10.1109/TAC.1977.1101446

Weghe, M. V., Rogers, M., Weissert, M., & Matsuoka, Y. (2004). The ACT hand: Design of the skeletal structure. In *Proceedings of the IEEE International Conference on Robots & Automation*. IEEE.

Yagiz, N., Arslan, Y. Z., & Hacioglu, Y. (2007). Sliding mode control of a finger for a prosthetic hand. *Journal of Vibration and Control*, *13*(6), 733–749. doi:10.1177/1077546307072352

Yagiz, N., & Hacioglu, Y. (2009). Robust control of a spatial robot using fuzzy sliding modes. *Mathematical and Computer Modelling*, *49*(1-2), 114–127. doi:10.1016/j.mcm.2008.05.050

Yagiz, N., Hacioglu, Y., & Arslan, Y. Z. (2010). Load transportation by dual arm robot using sliding mode control. *Journal of Mechanical Science and Technology*, *24*(5), 1177–1184. doi:10.1007/s12206-010-0312-9

Zadeh, L. A. (1965). Fuzzy sets. *Information and Control*, *8*(3), 338–353. doi:10.1016/S0019-9958(65)90241-X

Ziegler, J., & Nichols, N. (1942). Optimum settings for automatic controllers. *ASME Transactions*, *64*(3), 759–768.

KEY TERMS AND DEFINITIONS

Biomimetic Robot Hand: Human-made robot hands that imitate human nature.

Dexterous Manipulation: The ability of a manipulator to perform an action in an effective and skillful way.

Fuzzy Logic Control: A knowledge-based control method that is based on the fuzzy set theory.

Intelligent Control: Intelligent control is a class of control methods that use various artificial intelligence computing approaches.

PID Control: A classical control approach that sends the control signal to the plant which is equal to the proportional gain times the magnitude of the error e (difference between a measured process variable and a desired setpoint) plus the integral gain times the integral of the e plus the derivative gain times the derivative of the e.

Robust Control: Robust control is a method which is particularly focusing on the implications of model uncertainty and external disturbances.

Sliding Mode Control: A special class of variable structure control systems in which the control law is deliberately changed during the control process according to some predefined rules depending on the states of the system. It is known with its robust behavior.

APPENDIX 1

Table 4. Numerical parameters for the finger model

Parameter	Numerical Value	Unit	Parameter	Numerical Value	Unit
m_1	0.0027	[kg]	L_2	0.019	[kgm^2]
m_2	0.0013	[kg]	L_3	0.017	[kgm^2]
m_3	0.0005	[kg]	a	0.0185	[m]
$b_1 = b_2 = b_3$	0.0001	[Nms]	b	0.0095	[m]
M_1	0.0027	[kg]	c	0.0085	[m]
M_2	0.0010	[kg]	μ	0.001	[Nm]
M_3	0.0004	[kg]	m_{f1}	0.0009	[Nm]
I_1	3.1693 x 10^{-7}	[kg]	m_{f2}	0.0006	[Nm]
I_2	3.3003 x 10^{-8}	[kg]	m_{f3}	0.0003	[Nm]
I_3	1.0181 x 10^{-8}	[kg]	m_a	100	[s^{-1}]
L_1	0.037	[kgm^2]	m_t	1.37	[s]

APPENDIX 2

Mass Matrix $[M(\theta)]$**:**

$$[M(\theta)] = \begin{bmatrix} A_1 + A_2 + A_3 + 2L_1A_4c_2 + 2cM_3\left(L_1c_{23} + L_2c_3\right) \\ A_2 + A_3 + L_1A_4c_2 + cM_3\left(L_1c_{23} + 2L_2c_3\right) \\ A_3 + cM_3\left(L_1c_{23} + L_2c_3\right) \\ \\ A_2 + A_3 + L_1A_4c_2 + cM_3\left(L_1c_{23} + 2L_2c_3\right) \\ A_2 + A_3 + 2cM_3L_2c_3 \\ A_3 + cM_3L_2c_3 \\ \\ A_3 + cM_3\left(L_1c_{23} + L_2c_3\right) \\ A_3 + cM_3L_2c_3 \\ A_3 \end{bmatrix}$$

Coriolis and Centrifugal Vector $\mathbf{C}(\theta,\dot{\theta})$**:**

$$\boldsymbol{C}(\theta,\dot{\theta}) = \begin{bmatrix} b_1\dot{\theta}_1 - L_1\left(A_4s_2 + cM_3s_{23}\right)\left(2\dot{\theta}_1\dot{\theta}_2 + \dot{\theta}_2^2\right) - cM_3\left(L_1s_{23} + L_2s_3\right)\left(2\dot{\theta}_1\dot{\theta}_3 + 2\dot{\theta}_2\dot{\theta}_3 + \dot{\theta}_3^2\right) \\ b_2\dot{\theta}_2 + L_1\left(A_4s_2 + cM_3s_{23}\right)\dot{\theta}_1^2 - cM_3L_2s_3\left(2\dot{\theta}_1\dot{\theta}_3 + 2\dot{\theta}_2\dot{\theta}_3 + \dot{\theta}_3^2\right) \\ b_3\dot{\theta}_3 + cM_3\left(\left(L_1s_{23} + L_2s_3\right)\dot{\theta}_1^2 + L_2s_3\left(2\dot{\theta}_1\dot{\theta}_2 + \dot{\theta}_2^2\right)\right) \end{bmatrix}$$

Gravity Vector $\mathbf{G}(\theta)$**:**

$$\boldsymbol{G}(\theta) = \begin{bmatrix} g\left(A_5c_1 + A_6c_{12} + cM_3c_{123}\right) \\ g\left(A_6c_{12} + cM_3c_{123}\right) \\ gcM_3c_{123} \end{bmatrix}$$

Disturbance Torque Vector *F*:

$$\boldsymbol{F} = \begin{bmatrix} \tau_{d1} \\ \tau_{d2} + \tau_r \\ \tau_{d3} \end{bmatrix};\ \tau_{di} = \frac{m_{fi}}{1 + \exp(-m_a (t - m_t))}\ (i=1,2,3);\ \tau_r = \mu\, sign\ (\dot{\theta})$$

where

$$A_1 = M_1 a^2 + I_1 + (M_2 + M_3 + m_2 + m_3) L_1^2$$

$$A_2 = M_2 b^2 + I_2 + (M_3 + m_3) L_2^2$$

$$A_3 = M_3 c^2 + I_3$$

$$A_4 = M_2 b + (M_3 + m_3) L_2$$

$$A_5 = M_1 a + (M_2 + M_3 + m_2 + m_3) L_1$$

$$A_6 = M_2 b + (M_3 + m_3) L_2$$

The abbreviations used in above equations:

$$c_1 = \cos\theta_1,$$

$$s_2 = \sin\theta_2,$$

$$c_{123} = \cos\left(\theta_1 + \theta_2 + \theta_3\right),$$

$$s_{23} = \sin\left(\theta_2 + \theta_3\right).$$

APPENDIX 3

Table 5. Numerical values of the parameters for the designed controllers

PID		SMC		Fuzzy	
Parameter	**Numerical Value**	**Parameter**	**Numerical Value**	**Parameter**	**Numerical Value**
T_{I1}	0.5	τ_1	0.0006	SF_{e1}	2.5
T_{I2}	0.5	τ_2	0.0006	SF_{de1}	0.004
T_{I3}	0.5	τ_3	0.0006	SF_{e2}	2.5
T_{D1}	0.001	α_1	5	SF_{de2}	0.004
T_{D2}	0.001	α_2	5	SF_{e3}	2.5
T_{D3}	0.001	α_3	5	SF_{de3}	0.004
K_{P1}	0.1	Γ_1	200	SF_{u1}	0.2
K_{P2}	0.1	Γ_2	400	SF_{u2}	0.1
K_{P3}	0.01	Γ_3	800	SF_{u3}	0.03

APPENDIX 4

Table 6. Nomenclature

PID	Proportional-integral-derivative.
SMC	Sliding mode control.
FLC	Fuzzy logic control.
$[M(\theta)]$	Mass matrix.
$\mathbf{C}(\theta,\dot{\theta})$	Vector of Coriolis and centrifugal terms.
$\mathbf{G}(\theta)$	Gravity vector.
$\boldsymbol{u}$	Generalized torque vector.
$\boldsymbol{F}$	Vector of disturbance torques.
$\mathbf{x}$, $\dot{\mathbf{x}}$	Vector of state and its time derivative.
$\mathbf{e}$, $\dot{\mathbf{e}}$	Vector of error and its time derivative.
V	Lyapunov function.
σ	Sliding surface.
SF	Scaling factor.
IAE	Integral of Absolute Error.